A Bayesian Nonparametric Regression Model with Normalized Weights: A Study of Hippocampal Atrophy in Alzheimer's Disease

Isadora Antoniano-Villalobos [*] Sara Wade [†]

Stephen G. Walker [‡]

For the Alzheimer's Disease Neuroimaging Initiative. [§]

Abstract

Hippocampal volume is one of the best established biomarkers for Alzheimer's disease. However, for appropriate use in clinical trials research, the evolution of hippocampal volume needs to be well understood. Recent theoretical models propose a sigmoidal pattern for its evolution. To support this theory, the use of Bayesian nonparametric

[*] Bocconi University, Milan, Italy. PhD research funded by CONACyT

[†] University of Cambridge, Cambridge, UK.

[‡] University of Texas at Austin, USA.

[§] Data used in preparation of this article were obtained from the Alzheimer's Disease Neuroimaging Initiative (ADNI) database (`adni.loni.ucla.edu`). As such, the investigators within the ADNI provided data but did not participate in analysis or writing of this report. A complete listing of ADNI investigators can be found at: `http://adni.loni.ucla.edu/wp-content/uploads/how_to_apply/ADNI_Acknowledgement_List.pdf`.

regression mixture models seems particularly suitable due to the flexibility that models of this type can achieve and the unsatisfactory fit of semiparametric methods. In this paper, our aim is to develop an interpretable Bayesian nonparametric regression model which allows inference with combinations of both continuous and discrete covariates, as required for a full analysis of the data set. Simple arguments regarding the interpretation of Bayesian nonparametric regression mixtures lead naturally to regression weights based on normalized sums. Difficulty in working with the intractable normalizing constant is overcome thanks to recent advances in MCMC methods and the development of a novel auxiliary variable scheme. We apply the new model and MCMC method to study the dynamics of hippocampal volume, and our results provide statistical evidence in support of the theoretical hypothesis.

Keywords: Normalized weights; Dirichlet process mixture model; Latent model.

1 Introduction

Alzheimer's disease (AD) is an irreversible, progressive brain disease that slowly destroys memory and thinking skills, and eventually even the ability to carry out the simplest tasks (ADEAR, 2011). Due to its damaging effects and increasing prevalence, it has become a major public health concern. Thus, the development of disease-modifying drugs or therapies is of great importance.

In a clinical trial setting, with the purpose of assessing the effectiveness of any proposed drugs or therapies, accurate tools for monitoring disease progression are needed. Unfortunately, a definite measure of disease progression is unavailable, as even a definitive diagnosis requires histopathologic examination of brain tissue, an invasive procedure typically only performed at autopsy.

Non-invasive methods can be used to produce neuroimages and biospecimens which provide evidence of the changes in the brain associated with AD. Moreover, biomarkers based on neuroimaging or biological data may present a higher sensitivity to changes due to drugs or therapies over shorter periods of time than clinical measures, making them better suited tools for monitoring disease progression in clinical trials.

However, before biomarkers based on neuroimaging or biological data can be useful in clinical trials, their evolution over time needs to be well understood. Those which change earliest and fastest should be used as inclusion criteria for the trials and those which change the most in the disease stage of interest should be used for disease monitoring.

In this work, we focus on hippocampal volume, one of the best established neuroimaging biomarkers for AD. Jack et al. (2010), in a recent paper, propose a theoretical model for the evolution of hippocampal volume, which is further discussed in Frisoni et al. (2010). They hypothesize that hippocampal volume evolves sigmoidally with changes beginning early and continuing into late stages of the disease. This theoretical model needs to be validated, before the use of hippocampal volume as a measure for disease severity in clinical trials can be appropriately considered. Thus, in the present paper, we focus on the validation of Jack et al.'s proposed model.

Caroli and Frisoni (2010) and Sabuncu et al. (2011) assess the fit of parametric sigmoidal curves, and Jack et al. (2012) considers a more flexible model based on cubic splines with three chosen knot points. This last approach is the most flexible among the three, but they all impose significant restrictions which favor a sigmoidal shape. To provide strong statistical support for the sigmoidal shape hypothesis, a flexible nonparametric regression model is needed that would remove all restrictions on the regression curve allowing the data to choose the shape that provides the best fit.

There are many methods for nonparametric regression, and most standard approaches, such as splines, wavelets, or regression trees (Denison et al., 2002; Dimatteo et al., 2001), achieve flexibility by representing the regression function as a linear combination of basis functions. Another increasingly popular practice is to place a Gaussian process prior on the unknown regression function (Rasmussen and Williams, 2006).

While these models are able to capture a wide range of regression functions, the assumptions on the distribution of the errors about the mean is quite restrictrive; typically, independent and identically distributed additive Gaussian errors are assumed, and thus, these models are often referred to as semiparametric. In the hippocampal volume study, we not only expect a non linear behaviour for the evolution of the AD biomarker with age, but also suspect the presence of multimodality, heavy tails, and evolving variance in the error distribution due to variability in the onset of the disease and unobserved factors, such as enhanced cognitive reserve or neuroprotective genes. Indeed, in a semiparametric analysis of the data, we observe a non-normal behavior in the errors that depends on the covariates, which raises suspicions about the estimated regression curve.

To correctly model the data, a nonparametric approach for modelling the conditional density in its entirety is needed. In this way, no specific structure is imposed on the regression function or error distribution, so a fit confirming the hypothesized sigmiodal shape would provide strong statistical support for the theoretical model.

In this paper, we investigate the dynamics of hippocampal volume as a function of age, disease status, and gender. To do so, we construct a flexible and interpretable nonparametric mixture model for the conditional density of hippocampal volume which incorporates both continuous and discrete covariates. Simple arguments regarding the interpretation of Bayesian nonparametric regression mixtures lead naturally to regression weights based on normalized sums. To overcome the difficulties in working with the intractable normalizing constant, a novel auxiliary variable Markov chain Monte Carlo (MCMC) scheme is developed. The novel model and MCMC algorithm are applied to study the behavior of hippocampal volume, and the results provide strong support for the theoretical model.

The layout of the paper is as follows. In Section 2 we describe the model and provide its unique provision of interpretability. In Section 3 we introduce the associated latent variables necessary for estimating the model via MCMC methods and allowing for us to handle both continuous and categorical covariates simultaneously. Section 4, and the Appendix, details the MCMC algorithm in its entirety for estimating the model, and in Section 5 we present a comprehensive simulation study outlining exactly and precisely how the model works and what it is capable of achieving. In Section 6 we present our main work which is the study of the data for Alzheimer's disease. Finally, Section 7 concludes with a discussion.

2 The regression model

For independent and identically distributed observations, a standard form of mixture model is given by

$$f_P(y) = \int K(y|\theta)\mathrm{d}P(\theta), \tag{1}$$

where $K(\cdot|\theta)$ is a parametric family of density functions defined on $\mathbb{Y}$ and P is a probability measure on the parameter space Θ.

In a Bayesian setting, this model is completed by a prior distribution on the mixing measure P. A common prior choice, a stick-breaking prior, makes P a discrete random measure, which can be represented as

$$P = \sum_{j=1}^{\infty} w_j \delta_{\theta_j},$$

for some atoms $\theta_j \in \Theta$, taken i.i.d. from some probability measure P_0, known as the base measure; and weights $w_j \geq 0$, such that $\sum_j w_j = 1$ (a.s.), constructed from a sequence $v_j \overset{ind}{\sim} \mathrm{Beta}(\zeta_{1,j}, \zeta_{2,j})$ with $w_j = v_j \prod_{j'<j}(1 - v_{j'})$. The mixture model (Lo, 1984) can then be expressed as a countable convex combination of kernels

$$f_P(y) = \sum_{j=1}^{\infty} w_j K(y|\theta_j).$$

For the covariate dependent density estimation problem in which we are interested, the mixture model (1) can be adapted by allowing the mixing distribution P_x to depend on the covariate x and replacing the density model $K(y|\theta)$ with a regression model $K(y|x, \theta)$, such as a linear model. Hence, for every $x \in \mathbb{X}$,

$$f_{P_x}(y|x) = \int K(y|x, \theta)\mathrm{d}P_x(\theta).$$

Once again, the Bayesian model is completed by assigning a prior distribution on the family $\{P_x\}_{x\in\mathbb{X}}$ of covariate dependent mixing probability measures. If the prior gives probability one to the set of discrete probability measures, then

$$P_x = \sum_{j=1}^{\infty} w_j(x)\delta_{\theta_j(x)}, \quad \text{and} \quad f_{P_x}(y|x) = \sum_{j=1}^{\infty} w_j(x)K(y|x,\theta_j(x)), \tag{2}$$

where $\theta_j(x) \in \Theta$, and the $w_j(x) \geq 0$ are such that $\sum_j w_j(x) = 1$ (a.s.) for all $x \in \mathbb{X}$.

This general model was introduced by MacEachern (1999; 2000), who focused on the case when the weights are constant functions of x, $w_j(x) = w_j$, defined in accordance with a Dirichlet process (DP). Such simplified versions of the model are popular, as inference can be carried out using any of the well established algorithms for DP mixture models (see e.g. Neal, 2000; Papaspiliopoulos and Roberts, 2008; Kalli et al., 2011).

Recent developments explore the use of covariate dependent weights. To simplify computations and ease interpretation, atoms are usually assumed not to depend on the covariates. The main constraint for prior specification, in this case, is the condition, $\sum_j w_j(x) = 1$ for all $x \in \mathbb{X}$, which is non trivial for an infinite number of positive weights.

The only technique currently in use for directly defining the covariate dependent weights is through the stick-breaking representation, given by

$$w_1(x) = v_1(x) \text{ and for } j > 1 \quad w_j(x) = v_j(x)\prod_{j'<j}(1 - v_{j'}(x)), \tag{3}$$

where the $\{v_j(\cdot)\}$ are independent processes on $\mathbb{X}$ and independent of the atoms, $\{\theta_j\}$. There are various proposals for the construction of the $v_j(x)$, see e.g. Griffin and Steel (2006); Dunson and Park (2008); Rodriguez and Dunson (2011); Chung and Dunson (2009); Ren et al. (2011); or Dunson (2010) and Müller and Quintana (2010) for reviews of nonparametric regression mixture models.

The stick-breaking definition poses challenges in terms of the various choices that need to be made for functional shapes and hyper–parameters when defining the $\{v_j(x)\}$. The difficulties are amplified by the lack of interpretation of the quantities involved.

Moreover, combining continuous and discrete covariates in a useful way is far from straightforward.

We propose a different construction of the covariate dependent weights, which follows from an alternative perspective on mixture models. The idea is to realize that each weight contains information about the relative applicability of each parametric component, within the sample space $\mathbb{Y}$. In a regression setting, covariate dependent weights are necessary because it is not reasonable to assume that such relative importance is equal throughout the entire covariate space $\mathbb{X}$; rather, it depends on the value x. Since the nature of such dependence is unknown, the uncertainty about it should be incorporated through prior specification.

In the nonparametric mixture model

$$f_{P_x}(y|x) = \sum_{j=1}^{\infty} w_j(x) K(y|x, \theta_j),$$

each covariate dependent weight $w_j(x)$ represents the probability that an observation with a covariate value of x comes from the j^{th} parametric regression model $K(y|x, \theta_j)$. Thus, letting d be the random variable indicating the component from which an observation is generated, we have that $w_j(x) = p(d = j|x)$. A simple application of Bayes theorem implies

$$p(d = j|x) \propto p(d = j)p(x|d = j),$$

where $p(d = j)$ represents the probability that an observation, regardless of the value of the covariate, comes from parametric regression model j; and $p(x|d = j)$ describes how likely it is that an observation generated from regression model j has a covariate value of x.

Therefore, $p(x|d = j)$ can be defined to reflect prior beliefs as to where in the covariate space the regression model j will have the largest relative applicability. A natural and simple way to achieve this is to define it through a parametric kernel function $K(x|\psi_j)$ and with some prior on the ψ_j. Uncertainty about the $p(d = j) := w_j$ is expressed through a prior on the infinite dimensional simplex.

Putting things together, and incorporating the normalizing constant, we have that

$$w_j(x) = \frac{w_j K(x|\psi_j)}{\sum_{j'=1}^{\infty} w_{j'} K(x|\psi_{j'})}, \tag{4}$$

where $0 \leq w_j \leq 1$ for all j and $\sum_{j=1}^{\infty} w_j = 1$.

Note that the conditional densities $p(x|j)$ are not related to whether the covariates are picked by an expert or sampled from some distribution, which itself could be known or unknown. They only indicate priors about where, in $\mathbb{X}$, regression model j best applies. Moreover, the density $p(x) = \sum_{j=1}^{\infty} P(j)\, p(x|j)$ does not correspond to the distribution from which the covariates are sampled, if indeed they are sampled; it simply represents the likelihood that an observation has a covariate value of x.

The key element left to define is $K(x|\psi_j)$. If x is a continuous covariate, a natural choice is the normal density function. In this case, the interpretation would be that there is some central location $\mu_j \in \mathbb{X}$ where regression model j applies best, and a parameter τ_j describing the rate at which the applicability of the model decays around μ_j. On the other hand, if x is discrete, then a standard distribution on discrete spaces can be used, such as the Bernoulli or its generalization, the categorical distribution. Even if x is a combination of both discrete and continuous covariates, it is still possible to specify a joint density by combining both discrete and continuous distributions. This will be explained and demonstrated later on in the paper.

It is to be noted that the infinite sum in the denominator of (4) introduces an intractable normalizing constant for which no posterior simulation methods are currently available. Only finite versions of this type of model have been introduced in the literature (see e.g. Pettitt et al., 2003; Møller et al., 2006; Murray et al., 2006; Adams et al., 2008), since simulation methods are available only for the finite case. In the next section, we introduce a suitable set of latent variables, that solves the infinite dimensional intractable normalizing constant problem.

3 The latent model

The aim of this section is to re-express the model in terms of latent variables, which are essential for Bayesian inference. For a sample $\big((y_1, x_1), \ldots, (y_n, x_n)\big)$, the likelihood for the proposed model is given by

$$f_P(y_{1:n} \,|\, x_{1:n}) = \prod_{i=1}^{n} \left(\sum_{j=1}^{\infty} w_j(x_i)\, K(y_i|x_i, \theta_j) \right), \tag{5}$$

with covariate dependent weights given by expression (4). The infinite sum in the denominator constitutes an intractable normalizing constant, which makes inference infeasible. However, through a simple trick, which relies on the series expansion,

$$\sum_{k=0}^{\infty} (1-r)^k = r^{-1}, \text{ for } 0 < r < 1, \tag{6}$$

we can move the infinite sum from the denominator to the numerator, thus making inference possible, following the introduction of auxiliary variables.

In order to illustrate the ideas with a simplified notation, we start by considering the likelihood of a single data point. We assume the first q elements of x represent discrete covariates, each x_h taking values in $\{0, \ldots, G_h\}$, for $h = 1 \ldots, q$; the last p elements of x represent continuous covariates. In this case, we have

$$K(y|x, \theta_j) = \mathrm{N}(y|X\beta_j, \sigma_j^2),$$

$$K(x|\psi_j) = \prod_{h=1}^{q} \mathrm{Cat}(x_h|\rho_{j,h}) \prod_{h=1}^{p} \mathrm{N}(x_{h+q}|\mu_{j,h}, \tau_h^{-1}),$$

where $\theta_j = (\beta_j, \sigma_j)$, $\psi_j = (\rho_j, \mu_j, \tau)$, $X = (1, x')$; and $\mathrm{Cat}(\cdot|\rho_h)$ represents the categorical distribution,

$$\mathrm{Cat}(x_h|\rho_h) = \prod_{g=0}^{G_h} \rho_{h,g}^{\mathbf{1}\,(x_h=g)}.$$

To simplify the expression, we make $\tau_j \equiv \tau$ for all j, but this restriction may be removed with some realistic assumptions on τ_j.

The likelihood of the single data point (y, x) may be written as

$$f_P(y \,|\, x) = \frac{1}{r(x)} \sum_{j=1}^{\infty} w_j K(x|\psi_j)\, K(y \,|\, x, \theta_j),$$

where

$$r(x) = \sum_{j=1}^{\infty} w_j \, K(x|\psi_j),$$

$$K(x|\psi_j) = \prod_{h=1}^{q+p} K(x_h|\psi_{j,h}),$$

and

$$K(x_h|\psi_{j,h}) = \begin{cases} \prod_{g=0}^{G_h} \rho_{h,g}^{\mathbf{1}\,(x_h=g)} & h = 1, \ldots, q \\ \\ \exp\{-\frac{1}{2}\tau_{h-q}(x_h - \mu_{j,h-q})^2\} & h = q+1, \ldots, q+p. \end{cases}$$

Notice that we have redefined the kernel function $K(x|\psi_j)$ by cancelling the precision term τ from the normal density, which appears both in the numerator and the denominator of the normalized weights expression. In this way, we guarantee that $0 < r(x) < 1$ for all $x \in \mathbb{X}$, so we can apply the series expansion (6) to write

$$\frac{1}{r(x)} = \sum_{k=0}^{\infty} \left[1 - \sum_{j=1}^{\infty} w_j \, K(x|\psi_j) \right]^k = \sum_{k=0}^{\infty} \left[\sum_{j=1}^{\infty} w_j (1 - K(x|\psi_j)) \right]^k .$$

The last equality relies on the fact that $\sum_{j=1}^{\infty} w_j = 1$ almost surely.

This trick allows us to move the infinite sum from the denominator to the numerator and equivalently express the likelihood as

$$f_P(y \,|\, x) = \sum_{j=1}^{\infty} w_j K(x|\psi_j)\, K(y \,|\, x, \theta_j) \sum_{k=0}^{\infty} \left[\sum_{j=1}^{\infty} w_j (1 - K(x|\psi_j)) \right]^k . \tag{7}$$

We therefore introduce a latent variable k taking values in $\{0, \ldots, \infty\}$, where the joint density of (y, k) given the model parameters is

$$f_P(y, k \,|\, x) = \sum_{j=1}^{\infty} w_j K(x|\psi_j)\, K(y \,|\, x, \theta_j) \left[\sum_{j=1}^{\infty} w_j (1 - K(x|\psi_j)) \right]^k ,$$

so that marginalizing over k, gives us back the original likelihood (7).

We can now deal with the mixture in the usual way, by introducing a latent variable d to indicate the mixture component to which a given observation is associated. Thus, we obtain

$$f_P(y, k, d \,|\, x) = w_d K(x|\psi_d)\, K(y \,|\, x, \theta_d) \left[\sum_{j=1}^{\infty} w_j (1 - K(x|\psi_j)) \right]^k .$$

For the remaining sum, we have the exponent k to consider. We first re-write this term as the product of k copies of the infinite sum,

$$f_P(y, k, d \,|\, x) = w_d K(x|\psi_d)\, K(y \,|\, x, \theta_d) \prod_{l=1}^{k} \sum_{j_l=1}^{\infty} w_{j_l} (1 - K(x|\psi_{j_l})),$$

and then, introduce k latent variables, $D_1, \ldots, D_k$, arriving at the full latent model

$$f_P(y, k, d, D \,|\, x) = w_d K(x|\psi_d)\, K(y \,|\, x, \theta_d) \prod_{l=1}^{k} w_{D_l} (1 - K(x|\psi_{D_l})).$$

It is easy to check that the original likelihood (7) is recovered by marginalizing over the d, k and $D = (D_1, \ldots, D_k)$.

For a sample of size $n \geq 1$ we simply need n copies of the latent variables. Therefore, the full latent model is given by

$$\begin{aligned} f_P(y_{1:n}, k_{1:n}, d_{1:n}, D_{1:n} \,|\, x_{1:n}) = \prod_{i=1}^{n} & w_{d_i} K(x_i|\psi_{d_i}) K(y_i \mid x_i, \theta_{d_i}) \\ & \prod_{l=1}^{k_i} w_{D_{l,i}} \left(1 - K(x_i|\psi_{D_{l,i}})\right) . \end{aligned} \tag{8}$$

Once again, we note that the original likelihood (5) can be easily recovered by marginalizing over the $d_{1:n}, k_{1:n}$, and $D_{1:n}$. However, the introduction of these latent variables makes Bayesian inference possible, via posterior simulation of the (w_j), the (θ_j) and the (ψ_j), as we show in the next section.

4 Posterior inference via MCMC

A prior for P, defined by a prior specification for the weights (w_j) and the parameters, (θ_j) and (ψ_j), completes the Bayesian model.

Our focus, for the prior on the weights (w_j), is on stick-breaking priors (Ishwaran and James (2001)). Therefore, for some positive sequence $(\zeta_{1,j}, \zeta_{2,j})_{j=1}^{\infty}$ and independent $v_j \sim \text{Beta}(\zeta_{1,j}, \zeta_{2,j})$ variables, we have

$$w_1 = v_1, \quad \text{and for } j > 1, \quad w_j = v_j \prod_{j' < j} (1 - v_{j'}).$$

Some important examples of this type of prior are the Dirichlet process, when $\zeta_{1,j} = 1$ and $\zeta_{2,j} = \zeta$ for all j; the Poisson-Dirichlet process, when $\zeta_{1,j} = 1 - \zeta_1$ and $\zeta_{2,j} = \zeta_2 + j\zeta_1$ for $0 \leq \zeta_1 < 1$ and $\zeta_2 > -\zeta_1$; and the two parameter stick-breaking process where $\zeta_{1,j} = \zeta_1$ and $\zeta_{2,j} = \zeta_2$ for all j.

To complete the prior specification, the (θ_j, ψ_j) are i.i.d. from some fixed distribution F_0 and independent from the (v_j). We define F_0 through its associated density f_0, which in this case is defined by the product of the following components,

$$\begin{aligned} f_0(\beta_j, \sigma_j^2) &= \text{N}(\beta_j \,|\, \beta_0, \sigma_j^2 C^{-1})\text{Ga}(1/\sigma_j^2 \,|\, \alpha_1, \alpha_2); \\ f_0(\mu_j, \tau) &= \prod_{h=1}^{p} \text{N}(\mu_{j,h} \,|\, \mu_{0,h}, (\tau_h c_h)^{-1})\text{Ga}(\tau_h \,|\, a_h, b_h); \\ f_0(\rho_j) &= \prod_{h=1}^{q} \text{Dir}(\rho_{j,h} \,|\, \gamma_h). \end{aligned}$$

Together with the joint latent model, this provides a joint density for all the variables which need to be sampled for posterior estimation, i.e. the $(w_j, \theta_j, \psi_j, k_i, d_i, D_{l,i})$.

However, there is still an issue due to the infinite choice of the $(d_i, D_{l,i})$, which we overcome through the slice sampling technique of Kalli et al. (2011). Accordingly, in order to reduce the choices represented by $(d_i, D_{l,i})$ to a finite set, we introduce new latent variables, $(\nu_i, \nu_{l,i})$, which interact with the model through the indicating functions $\mathbf{1}\big(\nu_i < \exp(-\xi d_i)\big)$ and $\mathbf{1}\big(\nu_{l,i} < \exp(-\xi D_{l,i})\big)$, for some $\xi > 0$. Hence, the full conditional distributions for the index variables are given by

$$\mathbb{P}(d_i = j|\cdots) \propto w_j \exp(\xi j)\, K(x_i|\psi_j) K(y_i \,|\, x_i, \theta_j)\, \mathbf{1}(1 \leq j \leq J_i),$$

$$\mathbb{P}(D_{l,i} = j|\cdots) \propto w_j \exp(\xi j)\, (1 - K(x_i|\psi_j))\; \mathbf{1}(1 \leq D_{l,i} \leq J_{l,i}),$$

where $J_i = \lfloor -\xi^{-1} \log \nu_i \rfloor; \quad J_{l,i} = \lfloor -\xi^{-1} \log \nu_{l,i} \rfloor$.

Let $J = \max_{l,i}\{J_i, J_{l,i}\}$. At any given iteration, the full conditional densities for the variables involved in the MCMC algorithm do not depend on values beyond J, so we only need to sample a finite number of the (ψ_j, θ_j, w_j).

The $(w_j)_{j=1}^J$ can be updated at each iteration of the MCMC algorithm in the usual way, that is, by making $w_1 = v_1$ and, for $j > 1$, $w_j = v_j \prod_{j'<j}(1 - v_{j'})$, where the (v_j) are sampled independently from Beta distributions with updated parameters (specified in the Appendix).

The variables involved in the linear regression kernel, that is, the (β_j, σ_j^2) are updated in the standard way, well known in the context of Bayesian regression. Since the normal-inverse gamma prior is conjugate, we simply need to sample from a normal-inverse gamma distribution with updated parameters, detailed in the Appendix.

The full conditional distribution for the $(\psi_j)_{j=1}^J$ seems somewhat more complicated, due to the additional product term in the latent model (expression 8), involving the latent variables (k_i) and $(D_{l,i})$. However, such a product can be easily transformed into a truncation term, by the introduction of additional latent variables. Thus, posterior simulation for the $(\psi_j)_{j=1}^J$ is achieved simply by sampling from standard truncated distributions with updated parameters, which can be easily calculated due to the conjugate prior choice. The details of this procedure, as well as the resulting updated parameters and truncations are presented in the Appendix. At this point, we only mention that the introduction of these additional latent variables does not pose a problem, since they are all conditionally independent given the $(\psi_j)_{j=1}^J$, and hence can be sampled in parallel, using the “parfor” routine in Matlab.

Finally, for the update of each k_i, we use ideas involving a version of reversible jump MCMC (see Green, 1995) introduced by Godsill (2001), to deal with the change of dimension in the sampling space. We start by proposing a move from k_i to k_i+1 with probability 1/2, and accepting it with probability

$$\min\left\{1, \sum_{j=1}^{J} w_j\left(1-K(x_i|\psi_j)\right)\right\}.$$

The evaluation of this expression requires the sampling of the additional index D_{i,k_i+1}, and we choose $D_{i,k_i+1}=j$ with probability proportional to $w_j\left(1-K(x_i|\psi_j)\right)$, for $j=1,\ldots,J$.

Similarly, if $k_i>0$, a move from k_i to k_i-1 is proposed with probability 1/2, and accepted with probability

$$\min\left\{1, \left[\sum_{j=1}^{J} w_j\left(1-K(x_i|\psi_j)\right)\right]^{-1}\right\}.$$

It is therefore possible to perform posterior inference for the nonparametric regression model proposed, via an MCMC scheme applied to the latent model. We have successfully implemented the method in Matlab (R2012a), and present some results in the next section.

In the following examples, the aim is prediction and predictive density estimation, which under the quadratic loss are, respectively, given by

$$\mathrm{E}[Y_{n+1}|y_{1:n},x_{1:n+1}] = \mathrm{E}\left[\sum_{j=1}^{\infty} w_j(x_{n+1})X_{n+1}\beta_j\Big|y_{1:n},x_{1:n}\right], \tag{9}$$

$$f(y_{n+1}|y_{1:n},x_{1:n+1}) = \mathrm{E}\left[\sum_{j=1}^{\infty} w_j(x_{n+1})\mathrm{N}(y|X_{n+1}\beta_j,\sigma_j^2)\Big|y_{1:n},x_{1:n}\right], \tag{10}$$

where and $X_{n+1}=(1,x'_{n+1})$; and the expectation is taken with respect to the posterior of (w_j,θ_j,ψ_j). MCMC estimates for this quantities are used, as specified in the Appendix.

5 Simulation Study

To demonstrate the ability of the model to recover a complex regression function with covariate dependent errors, we simulate $n = 200$ data points (depicted in Figure 1a) through the following formula,

$$x_i \overset{iid}{\sim} \mathrm{N}(\cdot|0, 2.5),,$$
$$y_i|x_i \overset{ind}{\sim} \mathrm{N}\left(\cdot \Big| \frac{5}{1-\exp(-x)}, \frac{1}{4} + \exp\left(\frac{x-6}{3}\right)\right).$$

Our model is given by

$$f_P(y|x) = \sum_{j=1}^{\infty} w_j(x) N(y|X\beta_j, \sigma_j^2),$$
$$w_j(x) = \frac{w_j \exp(-\tau/2(x-\mu_j)^2)}{\sum_{j'=1}^{\infty} w_{j'} \exp(-\tau/2(x-\mu_{j'})^2)}.$$

The prior for (w_j) and (θ_j, ψ_j) is described in Section 4. The prior choice for the (w_j) is a Dirichlet process, i.e. $\zeta_{1,j} = 1$. Rather than using a hyper-prior for the precision parameter, we fix it to be 1. Due to the unidentifiability of the weights, such a practice corresponds to the standard solution of fixing the location of one of the variables for models with identifiability issues. The unidentifiability of the weights arises from the fact that they are given by $w_j(x) \propto w_j K(x|\psi_j)$. We resolve this in the usual way by fixing the locations of the (w_j) rather than assigning a hyper-prior to the precision parameter. Note the model is fundamentally different from the usual DP mixture model, where the weights (w_j) are the weights, without any multiplicative factors. Hence in the DP model the use of a hyper-prior for the precision parameter is known to be important.

For the prior of (θ_j, ψ_j), we set

$$\beta_0 = (0, 5/8)'; \quad C^{-1} = \mathrm{diag}(9, 1/4); \quad \alpha_1 = 1; \quad \alpha_2 = 1;$$
$$\mu_0 = 0; \quad c = 1/8; \quad a = 1; \quad b = 1.$$

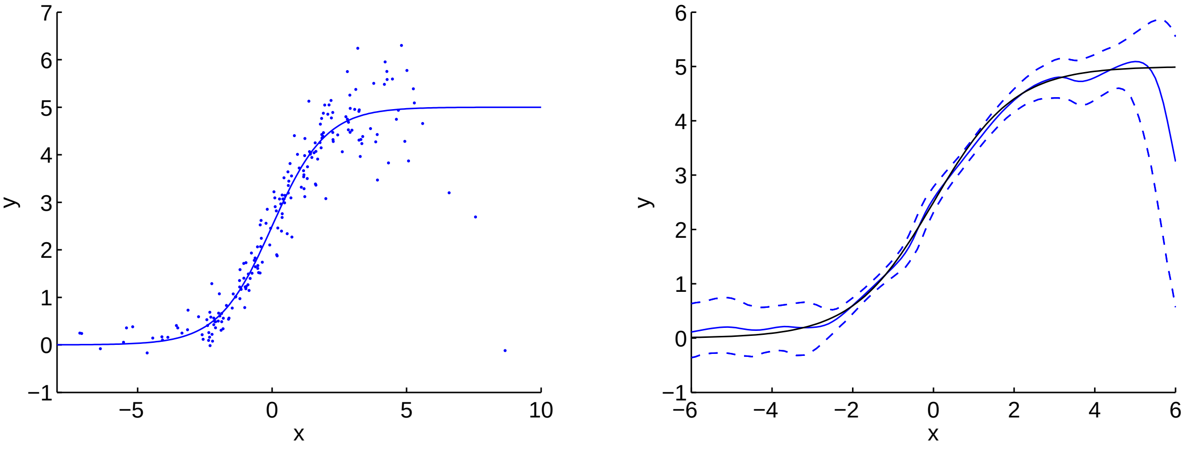

(a) Simulated data

(b) Predicted regression function

Figure 1: The left panel depicts the data and the true regression mean. The right panel depicts the estimated regression function (in blue) for a grid of new covariate values, along with 95% pointwise credible bands (dashed lines); the black line represents the true mean function.

Inference is carried out via the algorithm discussed in Section 4 with 5,000 iterations after a burn in period of 5,000.

Figure 1b depicts, in blue, the estimated regression function for a grid of unobserved x values, along with 95% pointwise credible bands. The true regression function is shown in black. Even though some extreme observations can be seen at the bottom right of Figure 1a, due to the exponential growth of the variance in the data-generating process, we can see that the shape of the regression function is recovered well and the true curve falls within the error bands. The effect of such extreme observations is only observed in the increase of the variance in the posterior distribution of the mean curve.

The flexibility in estimating the regression function relies heavily on the posterior distribution of the covariate dependent weights. The left panel of Figure 2 depicts the partition with highest estimated posterior probability, with data points coloured by

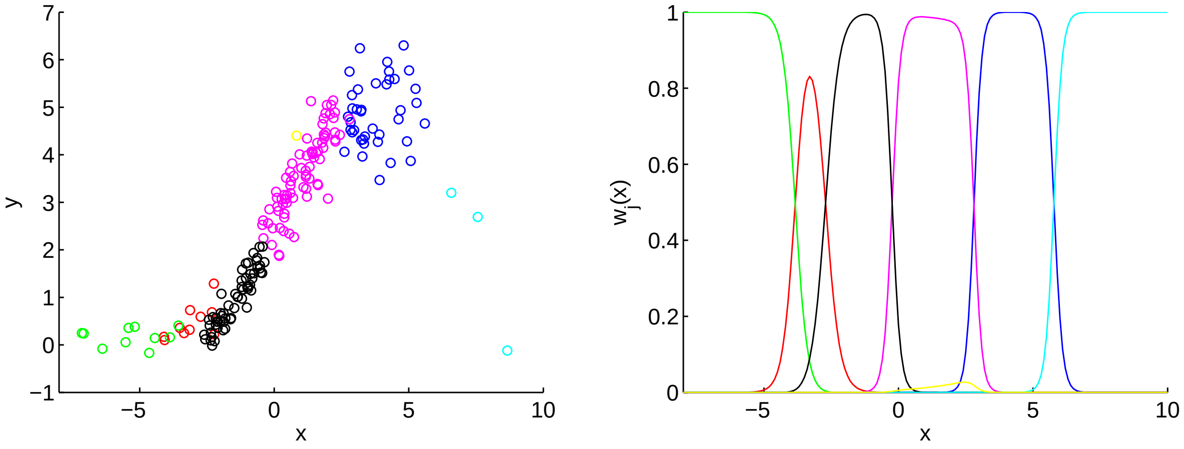

(a) Partition with highest prob.

(b) Covariate-dependent weights

Figure 2: The left panel depicts the partition with the highest posterior probability, where the data are colored by component membership. The right panel depicts the covariate-dependent weights associated to this partition.

component membership. The right panel of Figure 2 shows a posterior sample of the covariate-dependent weights as a function of x, given this partition. It is important to observe that *aposteriori* the weights are able to peak close to one in areas of high applicability of their associated linear regression models and decay smoothly or sharply, as needed, when the covariates move away from this area. For example, for values of x around 4 (blue cluster), a single linear regression model dominates; for values around -3 (red cluster), the dominance is less clear; while, for values around -4 a combined effect of two linear models is indicated by the dependent weights. The role of these dependent weights is essential to the interpolation capabilities of the model in regions of the covariate space where few observations are available. At the same time, the flexibility of the dependent weights ensures that the transition between regions of applicability of each linear model can be smooth or sharp, as required by the data. This clearly shows that the mixture of kernels involving the covariates in the denominator of normalized weights expression, is not modelling the structure of the covariate space, but only the regions in which each parametric linear model applies.

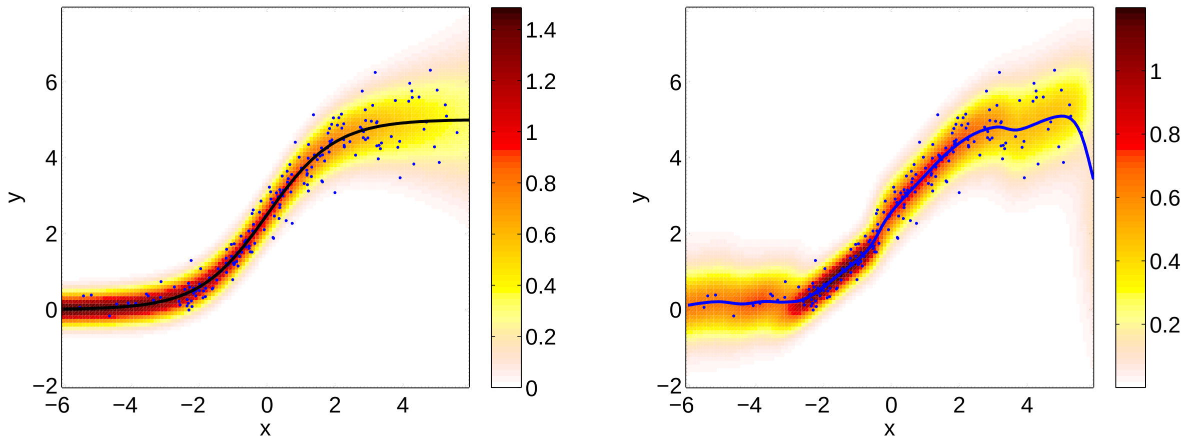

(a) True conditional densities

(b) Estimated conditional densities

Figure 3: The left panel depicts a heat plot of the true conditional densities $f(y|x)$ for a grid of covariate values; the right panel shows posterior estimates of such conditional densities. In both cases, the corresponding mean curve is shown in blue, along with the data.

We are also able to produce estimates of the full conditional density $f(y|x)$ at any value of x in the covariate space. These are also referred to as predictive densities. Results are shown in Figure 3b. The estimated densities are represented through heat maps, where a darker color indicates higher density values. The estimated densities can be compared with the true conditional densities, shown in Figure 3a. As is expected, the estimated variance is higher than the true in regions of the covariate space where less data is observed. However, it is clear from the picture that the exponential growth of the variance of $y|x$, as x changes, is recovered by the model. The simultaneous change in location and precision of the estimated conditional densities, for different values of the covariate can be better appreciated in Figure 4.

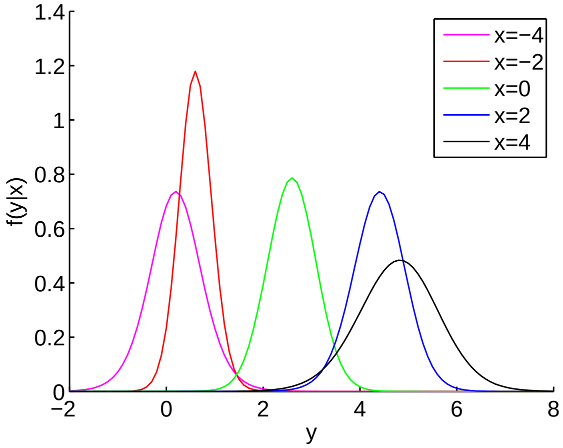

Figure 4: Estimated conditional densities, i.e. the predictive densities, $f(y|x)$ for five covariate values.

6 Alzheimer's disease study

Hippocampal volume is one of the best established and most studied biomarkers because of its known association with memory skills and relatively easy identification in sMRI. In two recent papers, Jack et al. (2010) and Frisoni et al. (2010) discussed a hypothetical model for the dynamics of hippocampal volume as a function of age and disease severity. If confirmed, this model would have important implications for the use hippocampal volume to measure the efficacy of treatments in clinical trials.

The clinical stages of the AD are divided into three phases (Jack et al. (2010)); the pre-symptomatic phase, prodromal phase, and the dementia phase. During the pre-symptomatic phase, some AD pathological changes are present, but patients do not exhibit clinical symptoms. This phase may begin possibly 20 years before the onset of clinical symptoms. The pre-prodromal stage of AD is known as mild cognitive impairment (MCI); patients diagnosed with MCI exhibit early symptoms of cognitive impairment, but do not meet the dementia criteria. The final stage of AD is dementia, when patients are officially diagnosed AD.

Jack et al. (2010) and Frisoni et al. (2010) hypothesized that hippocampal volume evolves sigmoidally over time, with changes starting slightly before the MCI stage and occurring until late in dementia phase. The steepest changes are supposed to occur shortly after the dementia threshold has been crossed.

To provide validation for this model, we study the evolution of hippocampal volume as a function of age, gender, and disease status. Data was obtained from the Alzheimer's Disease Neuroimaging Initiative database which is publicly accessible at UCLA's Laboratory of Neuroimaging[1]. The ADNI database contains neuroimaging, biological, and clinical data, along with summaries of neuroimages, including the volume of various brain structures. The dataset analysed here consists of the volume

[1] The ADNI was launched in 2003 by the National Institute on Aging (NIA), the National Institute of Biomedical Imaging and Bioengineering (NIBIB), the Food and Drug Administration (FDA), private pharmaceutical companies and non-profit organizations, as a \$ 60 million, 5-year public- private partnership. The primary goal of ADNI has been to test whether serial magnetic resonance imaging (MRI), positron emission tomography (PET), other biological markers, and clinical and neuropsychological assessment can be combined to measure the progression of mild cognitive impairment (MCI) and early Alzheimer's disease (AD). Determination of sensitive and specific markers of very early AD progression is intended to aid researchers and clinicians to develop new treatments and monitor their effectiveness, as well as lessen the time and cost of clinical trials. The Principal Investigator of this initiative is Michael W. Weiner, MD, VA Medical Center and University of California-San Francisco. ADNI is the result of efforts of many co-investigators from a broad range of academic institutions and private corporations, and subjects have been recruited from over 50 sites across the U.S. and Canada. The initial goal of ADNI was to recruit 800 adults, ages 55 to 90, to participate in the research, approximately 200 cognitively normal older individuals to be followed for 3 years, 400 people with MCI to be followed for 3 years and 200 people with early AD to be followed for 2 years. For up-to-date information, see `www.adni-info.org`.

hippocampus obtained from the sMRI performed at the first visit for 736 patients. Of the 736 patients in our study, 159 have been diagnosed with AD, 357 have MCI, and 218 are cognitively normal (CN). Figure 5 displays the data.

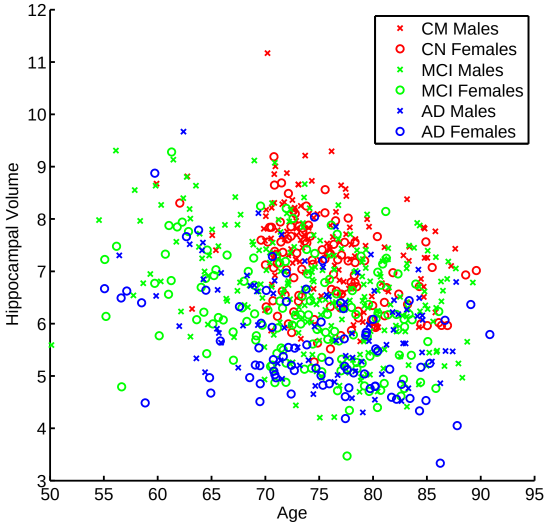

Figure 5: Hippocampal volume plotted against age. The data are colored by disease status with circles representing females and crosses representing males.

As discussed in Jack et al. (2010), we not only expect non-linearity in the regression function, but also suspect the possibility of non-normal and covariate dependent errors, for example due to the presence of unobserved neuroprotective genes. Indeed, in a preliminary semi-parametric analysis where the errors are assumed to be i.i.d. normal, we find some peculiarities in the model fit. Figures 6 and 7 display the estimated regression function and histogram of the errors within each combination of sex and disease status for the semi-parametric cubic spline and Gaussian process models, respectively, which are implemented in *crs* and *kernlab* packages in **R**. Notice that both of these models tend to overfit the data to overcome the rigid assumption on the errors. Furthermore, we find some abnormal behaviour in the errors that depends on

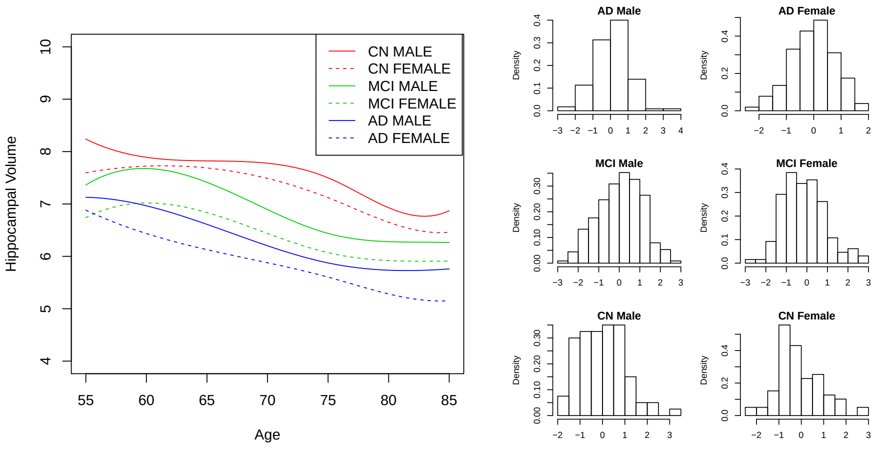

(a) Regression function

(b) Standardized errors

Figure 6: Cubic spline model: (6a) estimated regression function and (6b) histogram of the standardized errors as a function of sex and disease status.

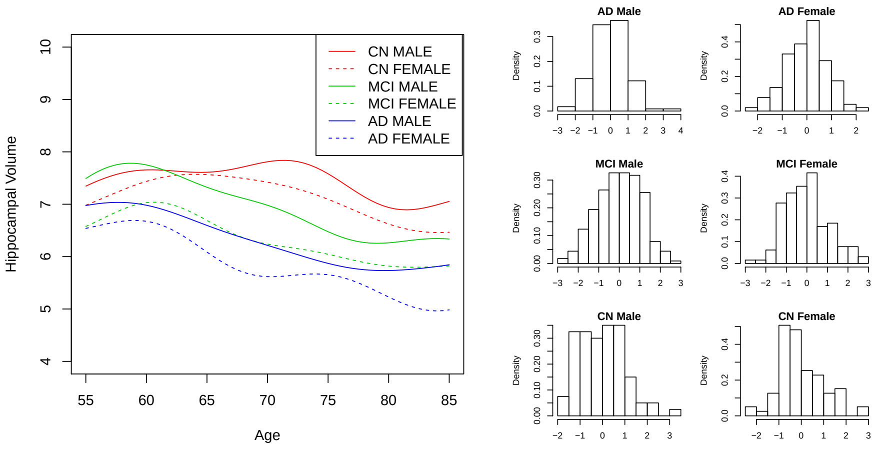

(a) Regression function

(b) Standardized errors

Figure 7: Gaussian process model: (7a) estimated regression function and (7b) histogram of the standardized errors as a function of sex and disease status.

sex and disease status. So, while the estimated mean function for the cubic splines looks reasonable and is similar to our own estimate (see Figure 8), the wrong error distribution about the mean will render prediction almost meaningless.

In order to fully capture the dynamics of the data, a nonparametric approach which flexibly models both the regression function and the error distribution is needed. To this aim, we consider the model developed in this paper, specifically, the infinite Gaussian kernel mixture model with covariate dependent weights given by

$$w_j(x) = \frac{w_j \prod_{h=1}^{2} \prod_{g=0}^{G_h} \rho_{j,h,g}^{1_{x_h=g}} \exp(-\tau/2(x_3-\mu_j)^2)}{\sum_{j'=1}^{\infty} w_{j'} \prod_{h=1}^{2} \prod_{g=0}^{G_h} \rho_{j',h,g}^{1_{x_h=g}} \exp(-\tau/2(x_3-\mu_{j'})^2)},$$

where $G_1 = 1$ (x_1 represents gender) and $G_2 = 2$ (x_2 represents disease status). Note that here age (x_3) is a real number measuring time from birth to exam date and thus, is treated as a continuous covariate. The prior distribution for w_j and (θ_j, ψ_j) is described in Section 4. The prior parameters for w_j are $\zeta_{1,j} = 1$ and $\zeta_{2,j} = 1$, corresponding to a Dirichlet process prior with a precision parameter of 1. See Section 5 for an explanation of this.

For the prior of (θ_j, ψ_j), we set

$$\beta_0 = (8, -1, -1, -1/4)'; \quad C^{-1} = \text{diag}(4, 1/4, 1/4, 1/50); \quad \alpha_1 = 1; \quad \alpha_2 = 1;$$
$$\gamma_1 = (1,1)'; \quad \gamma_2 = (1,1,1)'; \quad \mu_0 = 72.5; \quad c = 1/4; \quad a_1 = 1; \quad b_h = 1.$$

Inference is carried out via the algorithm discussed in Section 4 with 23,000 iterations after a burn in period of 7,000.

Figure 8 displays the estimated mean regression function for a grid of ages with all possible combinations of disease status and sex. Interestingly, we observe a confirmation of hypothesized sigmoidal evolution of hippocampal volume with increasing age. The estimated mean function coincides with the point predictor under the quadratic loss function. In this sense, cognitively normal subjects are predicted to have highest

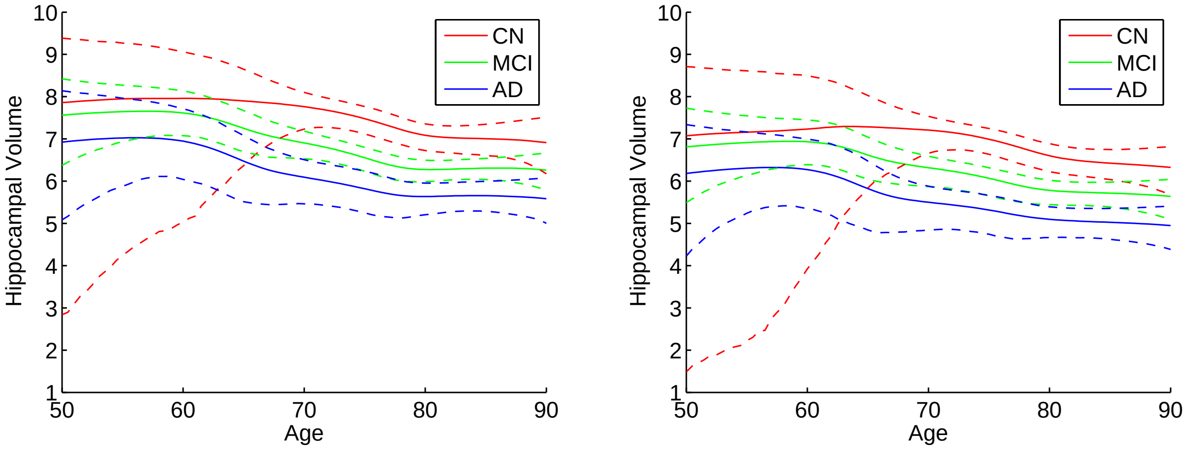

(a) Male patients

(b) Female patients

Figure 8: Estimated mean hippocampal volume as a function of age, disease, and sex. The curves are colored by disease status with dashed lines representing 95% pointwise credible intervals around the estimated regression function.

values of hippocampal volume at all ages, and MCI patients are predicted to have higher values of hippocampal volume at all ages when compared with AD patients. This indicates that hippocampal volume may be useful in disease staging during both the MCI and AD phases. With careful examination of Figure 8, we observe that CN patients are predicted to show the most gradual decline with increasing age, while AD patients display the greatest. Notice that, as expected, females are predicted to have lower values of hippocampal volume. We should comment that there is little data for the subgroup of CN subjects under 60, which reflects on the greater uncertainty in the estimation.

Figure 9 displays the heat map of conditional density estimates, i.e. the predictive densities, for a grid of new ages between 50 and 90 and all combinations of disease status and sex. In a clinical trial setting, the preference is for reliable outcome measures,

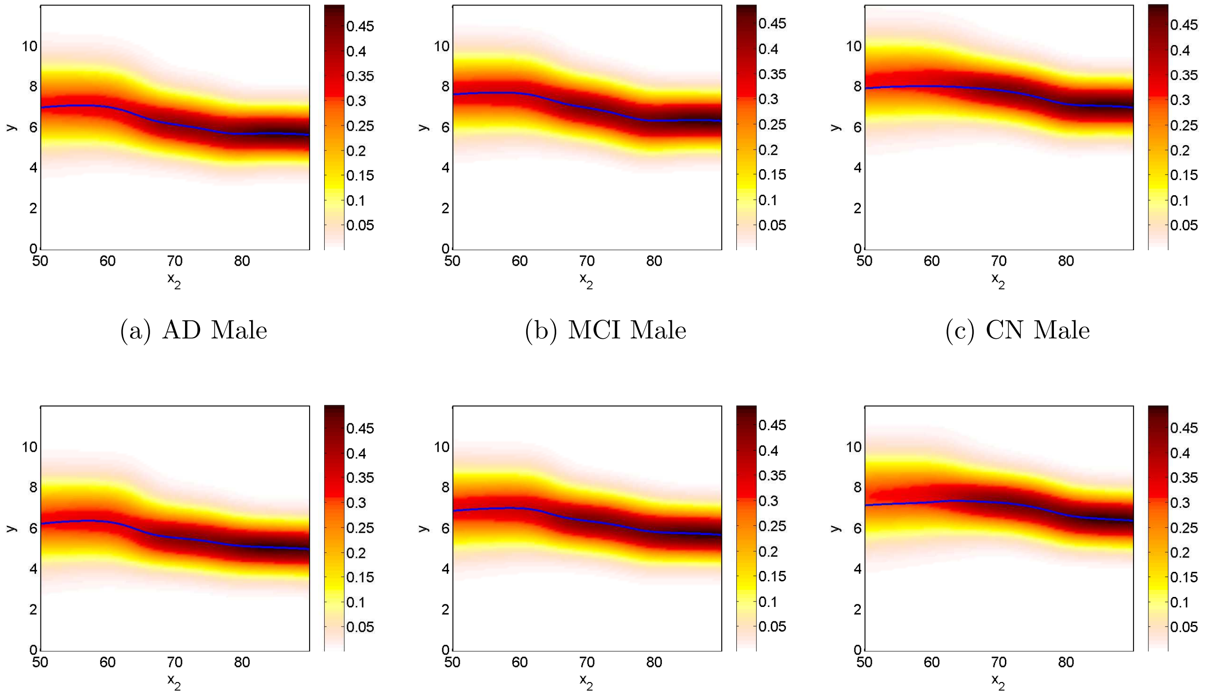

(a) AD Male

(b) MCI Male

(c) CN Male

(d) AD Female

(e) MCI Female

(f) CN Female

Figure 9: Heat map of conditional density estimates, i.e. predictve density, for new covariates with a grid of ages between 50 and 90 and all combinations of disease status and sex.

i.e. biomarkers with small variability. In general, we observe that variance decreases with increasing age, indicating that hippocampal volume is more reliable for elderly patients. The difference is slightly more pronounced for females as opposed to males. In particular, hippocampal volume is predicted to have a large variability for young females across all disease stages, with the largest for young CN females (the subgroup with no data). Instead, for older females, the variance is much smaller for all disease stages. When comparing males across disease status, we notice that young CN patients are predicted to show a large variability compared with young MCI and AD patients, while old MCI patients are predicted to show the largest variability when compared with their CN and AD counterparts.

This figure clearly illustrates a feature which provides a strong motivation for our model, rather than a simpler one which assumes constant variance and skewness, for example. The data suggest that it is important to model mean, variance, skewness and possibly also kurtosis as being dependent on the covariate values. Hence, a standard model such as $y = m(x) + \sigma\varepsilon$, $\varepsilon \overset{iid}{\sim} \mathrm{N}(0, 1)$ will fail to reproduce the results we have obtained for the more general $f(y|x)$ model. Even though the model is necessarily more complicated, all the elements in it are interpretable.

7 Discussion

In this paper, we have described and implemented a fully Bayesian nonparametric approach to examine the evolution of hippocampal volume as a function of age, gender, and disease status. We find that with increasing age, hippocampal volume is predicted to display a sigmoidal decline for cognitively normal, MCI, and AD patients. We also observe the most gradual decline for CN patients, while AD patients are predicted to show the steepest decline. As the approach was nonparametric, no structure was assumed for the regression function, yet our results confirm the hypothetical dynamics of hippocampal volume proposed by Jack et al. (2010). This provides strong statistical support for their model of hippocampal atrophy.

Future work in this application will involve examining the dynamics of various biomarkers jointly, which could be accomplished by replacing the normal linear regression component for y with a multivariate linear regression component. Another important future study will consist of combining the cross-sectional data with the longitudinal data for each patient.

In our analysis of the dynamics of hippocampal volume, we have developed a novel

Bayesian nonparametric regression model based on normalized covariate dependent weights. The important contributions of this approach are a natural and interpretable structure for the weights, a novel algorithm for exact posterior inference, and the inclusion of both continuous and discrete covariates.

We have focused on a univariate and continuous response, but the model and algorithm can be easily extended to accommodate other types of responses by, for example, simply replacing the normal linear regression component for y with a generalized linear model. Future work will consist of examining theoretical properties of this model.

Acknowledgments. Data collection and sharing for the Alzheimer's disease study was funded by the Alzheimer's Disease Neuroimaging Initiative (ADNI) (National Institutes of Health Grant U01 AG024904). We acknowledge the funding contributions of ADNI supporters (`adni-info.org/Scientists/ADNISponsors.aspx`).

The authors would like to thank the editor, associate editor and two referees for their valuable comments and suggestions on a previous submission of the paper.

Appendix

In this appendix, we specify the full conditional distributions for the MCMC posterior sampling scheme used for inference on the latent model constructed in section 3. Thus, the appendix constitutes a complement to section 4.

The sampling of the weights is obtained via the Stick Breaking definition, where the (v_j) must be independently sampled from the corresponding full conditionals,

$$f(v_j|\cdots) = \mathrm{Be}(\zeta_{1,j} + n_j + N_j, \zeta_{2,j} + n_j^+ + N_j^+),$$

where

$$n_j = \sum_i \mathbf{1}(d_i = j); \quad N_j = \sum_{l,i} \mathbf{1}(D_{l,i} = j);$$

$$n_j^+ = \sum_i \mathbf{1}(d_i > j); \quad N_j^+ = \sum_{l,i} \mathbf{1}(D_{l,i} > j).$$

Each of the (β_j, σ_j^2) can be sampled independently across j, from the full conditional density

$$f(\beta_j, \sigma_j^2 | \cdots) \;\; = \;\; \mathrm{N}(\beta_j \,|\, \hat{\beta}_j, \sigma_j^2 \hat{C}_j^{-1}) \mathrm{Ga}(1/\sigma_j^2 \,|\, \hat{\alpha}_{1j}, \hat{\alpha}_{2j}),$$

where $\quad \hat{\alpha}_{1j} = \alpha_1 + n_j/2; \qquad \hat{\alpha}_{2j} = \alpha_2 + \frac{1}{2}(\underline{y}_j - \underline{X}_j\beta_0)' W_j (\underline{y}_j - \underline{X}_j\beta_0);$

$$\hat{\beta}_j = \hat{C}_j^{-1}(C\beta_0 + \underline{X}_j' \underline{y}_j); \qquad \hat{C}_j = C + \underline{X}_j' \underline{X}_j; \qquad W_j = I_j - \underline{X}_j \hat{C}_j^{-1} \underline{X}_j'.$$

Here, $\underline{X}_j$ denotes the matrix with rows given by $X_i = (1, x_i')$ for $d_i = j$; $\underline{y}_j$ is defined analogously; and I_j denotes the identity matrix of size n_j.

We now show how the introduction of an additional set of latent variables enables the update of the $(\psi_j)_{j=1}^J$, as explained in section 4, and specify the resulting posterior densities and truncation regions.

Observe that, for any integer H and vector $(c_1, \ldots, c_H) \in (0,1)^H$, the following identity holds

$$1 - \prod_{h=1}^H c_h = \sum_{u \in \mathbb{U}} \int_{(0,1)^H} \prod_{h=1}^H \left[u_h \mathbf{1}\left(U_h < c_h\right) + (1 - u_h) \mathbf{1}\left(U_h > c_h\right) \right] \mathrm{d}U,$$

where $U = (U_1, \ldots, U_H)$, $u = (u_1, \ldots, u_H)$ and $\mathbb{U}$ is the set of H-dimensional $\{0,1\}$ vectors of which at least one entry is 0. We can, therefore, introduce latent variables $(u_{i,l,h}, U_{i,l,h})$, for $i = 1, \ldots, n$, $l = 1, \ldots, k_i$ and $h = 1, \ldots, q+p$, to deal with the terms $(1 - \prod_h K(x_{i,h}|\psi_{j,h}))$ in the latent likelihood (expression 8). The full conditional density for $(\psi_j)_{j=1}^J$ is thus extended to the latent expression

$$f(\psi_{1:J}, \{u_{i,l,h}\}, \{U_{i,l,h}\}| \cdots) \propto \prod_{j=1}^{J} f_0(\psi_j) \prod_{i=1}^{n} \prod_{h=1}^{q+p} K(x_{i,h}|\psi_{d_i,h})$$

$$\prod_{l=1}^{k_i} [u_{i,l,h} \mathbf{1}(U_{i,l,h} < K_{i,l,h}) + (1 - u_{i,l,h}) \mathbf{1}(U_{i,l,h} > K_{i,l,h})],$$

where $K_{i,l,h} = K(x_{i,h}|\psi_{D_{i,l},h})$, from which the original conditional density can be recovered by marginalizing over the $(u_{i,l,h}, U_{i,l,h})$.

The latent variables $(u_{i,l,h}, U_{i,l,h})$ can be sampled from their full conditional density by first observing that they are independent across $i = l, \ldots, n$ and $l = 1, \ldots, k_i$. For each i, l, the variable $u_{i,l}$ is a $q + p$-dimensional vector of zeros and ones with at least one zero entry. There are $2^{p+q} - 1$ such vectors, and for any u in this set, the update must be done according to the following distribution

$$\mathbb{P}(u_{i,l} = u| \cdots) \propto \prod_{h=1}^{q+p} \left[u_h K(x_{i,h}|\psi_{D_{i,l},h}) + (1 - u_h)(1 - K(x_{i,h}|\psi_{D_{i,l},h}))\right].$$

Conditional on $u_{i,l}$, the latent variables $U_{i,l,h}$ for $h = 1, \ldots, p + q$ are independent and uniformly distributed in the region

$$\left[K(x_{i,h}|\psi_{D_{i,l},h})(1 - u_{i,l,h}), K(x_{i,h}|\psi_{D_{i,l},h})^{u_{i,l,h}}\right].$$

Therefore, the additional variables do not pose a problem for posterior simulation. Furthermore, the introduction of these new variables transforms the latent term, introduced to deal with the intractable normalizing constant, into a product of truncation terms which is multiplied by the usual posterior density for the nonparametric mixture.

We first consider the update of the $(\rho_j)_{j=1}^J$, which is achieved by sampling each $\rho_{j,h}$ independently from a truncated Dirichlet distribution,

$$f(\rho_{j,h} \mid \cdots) \propto \text{Dir}(\rho_{j,h} \mid \hat{\gamma}_{j,h}) \mathbf{1}(\rho_{j,h} \in R_{j,h}),$$

where,

$$\hat{\gamma}_{j,h,g} = \gamma_{j,h,g} + \sum_{d_i=j} \mathbf{1}\,(x_{i,h} = g)\,.$$

The truncation region for each of the $(\rho_j)_{j=1}^{J}$ is given by

$$R_{j,h} = \left\{\rho \in (0,1)^{G_h} : r^{-}_{j,h,g} < \rho_g < r^{+}_{j,h,g},\ g = 1,\ldots,G_h\right\}$$

and for $g = 0\ldots,G_h$,

$$\begin{aligned} r^{-}_{j,h,g} &= \max\left\{U_{i,l,h}\mathbf{1}\,(x_{i,h} = g) : D_{i,l} = j, u_{i,l,h} = 1\right\}, \\ r^{+}_{j,h,g} &= \min\left\{U_{i,l,h}^{\mathbf{1}\,(x_{i,h}=g)} : D_{i,l} = j, u_{i,l,h} = 0\right\}. \end{aligned}$$

We then consider the $(\mu_j, \tau_j)_{j=1}^{J}$. Recall that $\tau_j = \tau$ for every j, so we update this variable by sampling each τ_h independently from a truncated gamma density,

$$f(\tau_h \,|\, \cdots) \propto \mathrm{Ga}(\tau_h \,|\, \hat{a}_h, \hat{b}_h)\mathbf{1}\,(\tau_h \in T_h),$$

where

$$\begin{aligned} \hat{a}_h &= a_h + J/2, \\ \hat{b}_h &= b_h + \frac{1}{2}\sum_{i=1}^{n}(x_{i,h+q} - \mu_{d_i,h})^2 + \frac{1}{2}c_h\sum_{j=1}^{J}(\mu_{j,h} - \mu_{0,h})^2. \end{aligned}$$

The truncation region for each τ_h is an interval $T_h = (\tau_h^{-}, \tau_h^{+})$, where

$$\begin{aligned} \tau_h^{-} &= \max\left\{\frac{-2\log U_{i,l,h+q}}{(x_{i,h+q} - \mu_{D_{i,l},h})^2} : u_{i,l,h+q} = 0\right\}, \\ \tau_h^{+} &= \min\left\{\frac{-2\log U_{i,l,h+q}}{(x_{i,h+q} - \mu_{D_{i,l},h})^2} : u_{i,l,h+q} = 1\right\}. \end{aligned}$$

We then sample each $\mu_{j,h}$ independently from a truncated normal

$$f(\mu_{j,h} \,|\, \cdots) \propto \mathrm{N}(\mu_{j,h} \,|\, \hat{\mu}_{j,h}, (\tau_h \hat{c}_{j,h})^{-1})\,\mathbf{1}\,(\mu_{j,h} \in A_{j,h})\,,$$

where

$$\hat{\mu}_{j,h} = \frac{1}{\hat{c}_{j,h}}\left(c_h\mu_{0,h} + \sum_{d_i=j} x_{i,h+q}\right); \quad \hat{c}_{j,h} = c_h + n_j.$$

The truncation region for each of the $\mu_{j,h}$ is an intersection of sets,

$$A_{j,h} = \bigcap_{D_{i,l}=j} A_{i,l,h},$$

where each $A_{i,l,h}$ is defined in terms of the intervals,

$$I_{i,l,h} = \left(x_{i,h+q} - \sqrt{\frac{-2\log U_{i,l,h+q}}{\tau_h}},\ x_{i,h+q} + \sqrt{\frac{-2\log U_{i,l,h+q}}{\tau_h}} \right),$$

as $A_{i,l,h} = I_{i,l,h}$ when $u_{i,l,h+p} = 1$, and $A_{i,l,h} = I^c_{i,j,h}$ when $u_{i,l,h+p} = 0$.

Finally, in order to improve the mixing of the algorithm we applied the label switching moves introduced by Papaspiliopoulos and Roberts (2008).

The Markov Chain scheme detailed here and explained in section 4, produces posterior samples $(w_j^s, \theta_j^s, \psi_j^s)$ for $s = 1, \ldots, S$, which can be used to estimate the regression mean (9) and predictive density (10) via

$$\mathrm{E}[Y_{n+1}|y_{1:n}, x_{1:n+1}] \approx \sum_{s=1}^{S}\sum_{j=1}^{J^s} w_j^s(x_{n+1})\underline{X}_{n+1}\beta_j^s,$$

$$f(y_{n+1}|y_{1:n}, x_{1:n+1}) \approx \sum_{s=1}^{S}\sum_{j=1}^{J^s} w_j^s(x_{n+1})\mathrm{N}(y|\underline{X}_{n+1}\beta_j^s, \sigma_j^{2s}),$$

where

$$w_j^s(x_{n+1}) = \frac{w_j^s K(x_{n+1}|\psi_j^s)}{\sum_{j'=1}^{J^s} w_{j'}^s K(x_{n+1}|\psi_{j'}^s)}.$$

References

R.P. Adams, I. Murray, and D.J.C. MacKay. Retrospective markov chain monte carlo methods for dirichlet process hierarchical models. *Biometrika*, 95:169–186, 2008.

Alzheimer's Disease Education & Referral Center ADEAR. Alzheimer's disease fact sheet. *NIH Publication*, 11-6423, 2011.

A. Caroli and G.B. Frisoni. The dynamics of Alzheimer's disease biomarkers in the Alzheimer's Disease Neuroimaging Initiative cohort. *Neurobiology of Aging*, 31:1263–1274, 2010.

Y. Chung and D.B. Dunson. Nonparametric Bayes conditional distribution modeling with variable selection. *Journal of the American Statistical Association*, 104:1646–1660, 2009.

D.G.T. Denison, C.C. Holmes, B.K. Mallick, and A.F.M Smith. *Bayesian Methods for Nonlinear Classification and Regression*. John Wiley & Sons, 2002.

I. Dimatteo, D.R. Genovese, and R.E. Kass. Bayesian curve fitting with free-knot splines. *Biometrika*, 88:1055–1071, 2001.

D. B. Dunson. *Nonparametric Bayes applications to biostatistics*, chapter 7, pages 223–273. Cambridge University Press, Cambridge, 2010.

D.B. Dunson and J.H. Park. Kernel stick-breaking processes. *Biometrika*, 95:307–323, 2008.

G.B. Frisoni, N.C. Fox, C.R. Jr Jack, P. Scheltens, and P.M. Thompson. The clinical use of structural MRI in Alzheimer disease. *Nature Reviews Neurology*, 6:67–77, 2010.

S.J. Godsill. On the relationship between Markov chain Monte Carlo Methods for model uncertainty. *Journal of Computational and Graphical Statistics*, 10(2):230–248, 2001.

P.J. Green. Reversible jump Markov chain Monte Carlo computation and Bayesian model determination. *Biometrika*, 82(4):711–732, 1995.

J.E. Griffin and M. Steel. Order-based dependent Dirichlet processes. *Journal of the American Statistical Association*, 10:179–194, 2006.

H. Ishwaran and L.F. James. Gibbs sampling methods for stick-breaking priors. *Journal of the American Statistical Association*, 96:161–173, 2001.

C.R. Jr Jack, D.S. Knopman, W.J. Jagust, L.M. Shaw, Aisen P.S., M.W. Weiner, R.C. Petersen, and J.Q. Trojanowski. Hypothetical model of dynamic biomarkers of the Alzheimer's pathological cascade. *Lancet Neurology*, 9:119–128, 2010.

C.R. Jr Jack, P. Vemuri, H.J. Wiste, S.D. Weigand, T.G. Lesnick, V. Lowe, K. Kantarci, M.A. Bernstein, M.L. Senjem, J.L. Gunter, B.F. Boeve, J.Q. Trojanowski, L.M. Shaw, P.S. Aisen, M.W. Weiner, R.C. Petersen, and D.S. Knopman. Shapes of the trajectories of 5 major biomarkers of Alzheimer disease. *Archives of Neurology*, 69: 856–867, 2012.

M. Kalli, J.E. Griffin, and S.G. Walker. Slice sampling mixture models. *Statistics and Computing*, 21:93–105, 2011.

A.Y. Lo. On a class of Bayesian nonparametric estimates: I. Density estimates. *The Annals of Statistics*, 12(1):351–357, 1984.

S.N. MacEachern. Dependent nonparametric processes. In *ASA Proceedings of the Section on Bayesian Statistical Science*, pages 50–55, Alexandria, VA, 1999. American Statistical Association.

S.N. MacEachern. Dependent dirichlet processes. *Technical Report, Department of Statistics, Ohio State University*, 2000.

J. Møller, A.N. Pettitt, R. Reeves, and K.K. Berthelsen. An efficient Markov chain Monte Carlo method for distributions with intractable normalising constants. *Biometrika*, 93(2):451–458, 2006.

P. Müller and F. Quintana. *More nonparametric Bayesian models for biostatistics*, chapter 8, pages 274–291. Cambridge University Press, Cambridge, 2010.

I. Murray, Z. Ghahramani, and D.J.C. MacKay. MCMC for doubly-intractable distributions. In *Proceedings of the 22nd Annual Conference on Uncertainty in Artificial Intelligence (UAI-06)*, pages 359–366. AUAI Press, 2006.

R.M. Neal. Markov chain sampling methods for Dirichlet process mixture models. *Journal of Computational and Graphical Statistcs*, 9:249–265, 2000.

O. Papaspiliopoulos and G.O. Roberts. Retrospective Markov chain Monte Carlo methods for Dirichlet process hierarchical models. *Biometrika*, 95(1):169–186, 2008.

A.N. Pettitt, N. Friel, and R. Reeves. Efficient calculation of the normalizing constant of the autologistic and related models on the cylinder and lattice. *Journal of the Royal Statistical Society: Series B (Statistical Methodology)*, 65(1):235–246, 2003.

C.E. Rasmussen and C.K.I. Williams. *Gaussian Processes for Machine Learning.* the MIT Press, 2006.

L. Ren, L. Du, D.B. Dunson, and L. Carin. The logistic stick-breaking process. *Journal of Machine Learning and Research*, 12:203–239, 2011.

A. Rodriguez and D.B. Dunson. Nonparametric Bayesian models through probit stick-breaking processes. *Bayesian Analysis*, 6:145–178, 2011.

M.R. Sabuncu, R.S. Desikan, J. Sepulcre, B.T.T. Yeo, H. Liu, N.J. Schmansky, M. Reuter, M.W. Weiner, R.L. Buckner, R.A. Sperling, and B. Fischl. The dynamics of cortical and hippocampal atrophy in Alzheimer disease. *Archives of Neurology*, 68:1040–1048, 2011.